AIAA SciTech
13-17 January 2014, National Harbor, Maryland
52nd Aerospace Sciences Meeting

Comparison of Pressures Driven by Repetitive Nanosecond Pulses to AC Result

Qi Chen[1], Xuanshi Meng[2], Bin Wu[3], Yushuai Wang[4]
(*1. National Key Laboratory of Science and Technology on Aerodynamic Design and Research, Northwestern Polytechnical University, Xi'an 710072, China*)

Feng Liu[5], Shijun Luo[6]
(*2. The Department of Mechanical and Aerospace Engineering , University of California, CA 92697-3975, America)*

This paper provides an attempt to measure the pressure distribution actuated by dielectric barrier discharge (DBD) actuator. The efficacy of DBD plasmas driven by repetitive nanosecond (NS) pulses for pressure distribution is investigated experimentally in quiescent air. The NS pulse driven DBD plasma actuator (NS-DBD hereafter, transfers very little momentum to the neutral air, so the value of induced velocity is far less than that of AC-DBD. Pressure distribution is measured by a PSI 9816 pressure scanner and ND-8 micro-pressure transmitters. For the result form PSI 9816, the convergences of time-averaged pressure increment components are verified. A parametric study on pressure distribution for NS-DBD is conducted for the max voltage value ranging from 6.88 kV to 9.8 kV at the carrier frequency of 1.712kHz in comparison with the results of AC-DBD conducted for the peak-peak 12.8kV at the carrier frequency of 11.75kHz.

Nomenclature

V	=	voltage of the sources
$V_{p\text{-}p}$	=	peak-to-peak voltage of a.c. voltage source, kV
V_{max}	=	max voltage of N.S. source, kV
F	=	control frequency of the sources, kHz
Δp	=	pressure increment from atmospheric pressure. Pa
t	=	time, s

I. Introduction

RECENTLY, plasma active flow control has received growing attention because of the advantages of that the actuator are entirely surface mounted, lack mechanical parts and possess high bandwidth wile requiring relatively low power. Dielectric Barrier Discharge (DBD) plasma actuators driven by AC waveforms (AC-DBD) are the most popular of these devices[1]. They have been widely used for controlling flow separation, particularly on the leading edge of airfoils in relatively low velocity freestreams (~30 m/s)[2]. The control mechanism for AC-DBD plasma actuators arises from an electrohydrodynamic (EHD) effect. Interaction between the charged species in the plasma and neutral particles near the surface generates a low speed (<10 m/s) near wall jet in quiescent air, thus limiting its application in practical flight environments. Efforts to extend the AC-DBD control authority continue to be explored through optimization of a single actuator, the use of multiple actuators and more novel arrangements like sliding discharges that rely on additional DC bias voltages[3-4]. The common goal in all these cases is to increase

[1] Graduate Student, Department of Fluid Mechanics.
[2] Associate Professor, Department of Fluid Mechanics.
[3] Graduate Student, Department of Fluid Mechanics.
[4] Graduate Student, Department of Fluid Mechanics.
[5] Professor, Department of Mechanical and Aerospace Engineering. Fellow AIAA.
[6] Researcher, Department of Mechanical and Aerospace Engineering.

the velocity generated by the device.

Early reports suggest DBD plasma actuators driven by a different type of waveform could be a superior alternative at high-speed. The construction of the device is analogous to the AC-DBD, but the discharge is driven by repetitive nanosecond duration pulses. DBD plasma created using these waveforms has shown control authority for leading edge airfoil separation control up to Mach 0.74 in an isolated publication.[5] This control authority is well beyond any reported results with AC-DBD plasma actuators on airfoils, but many questions such as the effect of wind tunnel blockage and the underlying flow physics remain unanswered. It should be noted that such waveforms have also been used in combination with AC and DC bias voltage[6-7].

In this paper an investigation on pressure distribution of the plasma is performed with the PSI 9816 pressure scanner. The convergences of time-averaged pressure increment components are verified. Distributions of pressure increment along lines parallel to coordinate axes are also displayed. Finally some conclusions and future work are presented.

II. Experimental Setup

A. Dielectric-Barrier-Discharge Plasma Actuator and Test Chamber

Dielectric Barrier Discharge (DBD) actuators as shown in Fig. 1 are used in the present research. The plasma actuator consists of two asymmetric copper electrodes each of 0.03 mm thickness. Seven Kapton tape layers (0.056 mm thick per layer) separate the encapsulated electrode from the exposed electrode. The effective span wise length(along which plasma is generated) is 200 mm. The width of the exposed and encapsulated electrode is 5 mm and 10mm, respectively. The two electrodes are separated by a gap of 0 mm, where the plasma is created and emits a blue glow in darkness.

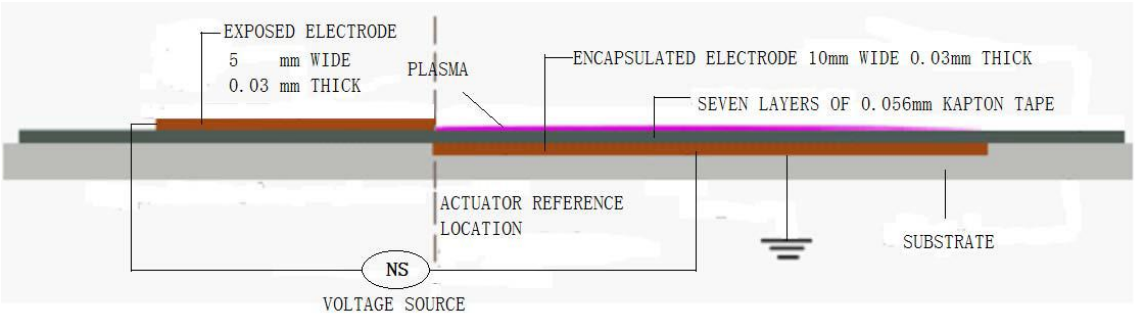

Figure 1. DBD plasma actuator schematic.

.

In order to reduce the effect of any external disturbances on the measurement, all tests are conducted in still air which is achieved by a closed cuboid chamber with a length of 600 mm, a width of 500 mm and a height of 500 mm. The bottom is the surface of a test table, and the other five faces of the chamber are made from plexiglas of 5 mm thick. The air inside the chamber under one atmospheric pressure is shielded from the air in the laboratory room.[8]

In our study, two kinds of sources are used. NS source are mainly used for the research for the max voltage values are set at V_{max}=6.88 kV/9.2kV/9.8 kV and the carrier frequency of 1.712 kHz. As a comparison, AC source are set at $V_{P\text{-}P}$=12kV and the carrier frequency of 11.8 kHz. An overview of the actuator parameters for all measurements is shown in Table 1.

Table 1. Actuator setup: dimensions and measured parameters.

Parameter	Value(s)			
Source	AC($V_{P\text{-}P}$)	NS(V_{max})		
Operating voltages (V, kV)	12	6.88	9.2	9.8
Operating frequency (F, kHz)	11.8	1.712		
Plasma actuator length (mm)	200			
Upper electrode width (copper, mm)	5			
Lower electrode width (copper, mm)	10			
Gap distance (mm)	0			
Dielectric thickness (Kapton, mm)	0.392			

B. Voltage and Glow of Repetitive Nanosecond Pulses and AC Voltage Source

Simultaneous measurements of voltage for NS-DBD plasma are shown in Fig. 2 a). An example of the same measurement for a typical AC-DBD plasma actuator is also provided for reference in Fig. 2 c). The NS-DBD pulse width is ~40ns and reaches peak voltage of ~14.5kV. The AC-DBD voltage trace is sinusoidal with a peak to peak voltage of ~15 kV and frequency of 11.75kHz.

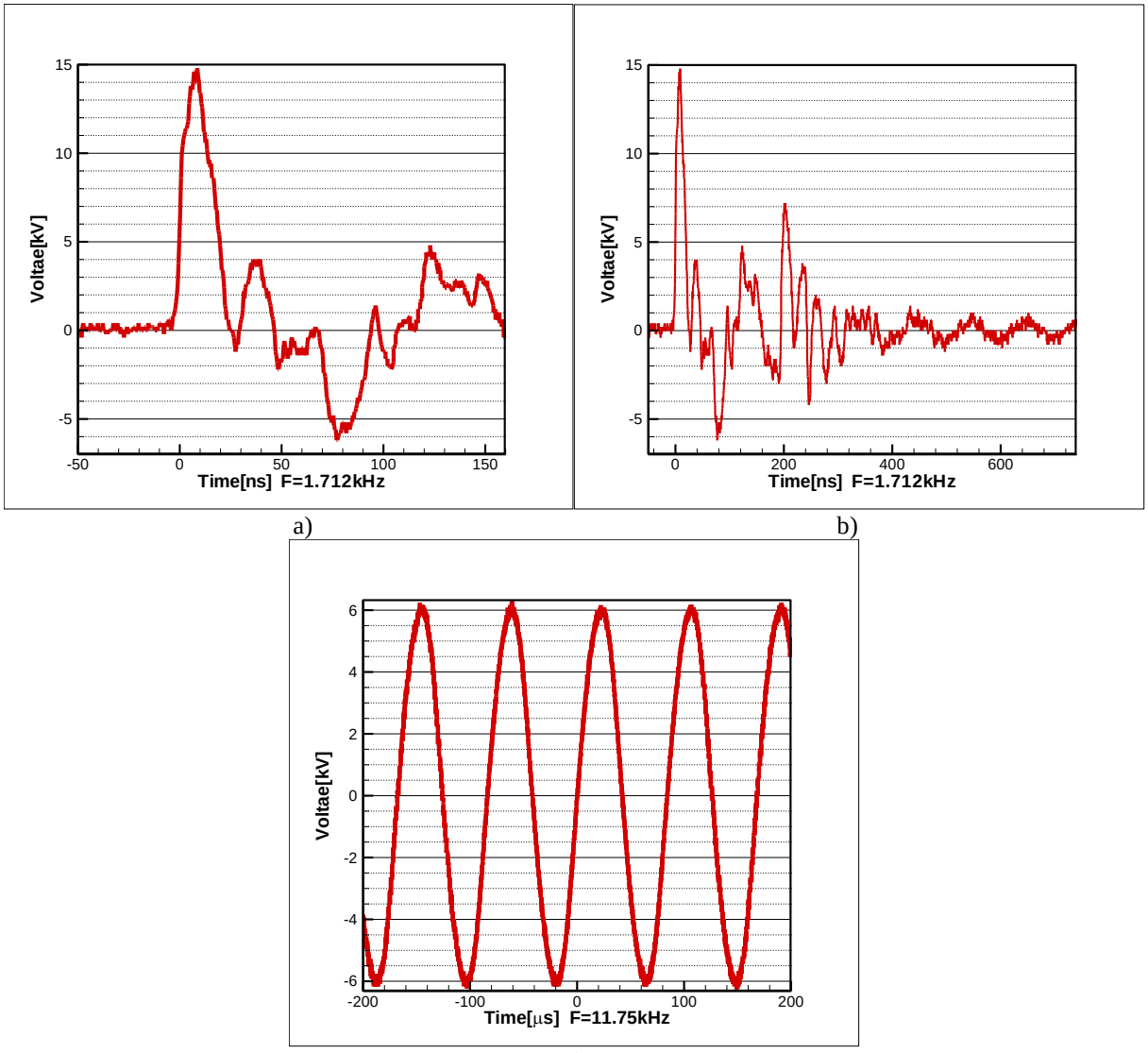

Figure 2. Voltage traces for NS-DBD a), b) and AC-DBD c) plasma actuators on a ~20 cm long DBD load.

The NS-DBD pulse width is ~50 ns and reaches peak voltage of ~14.5 kV. The AC-DBD voltage trace is sinusoidal with a peak to peak voltage of ~12.4 kV and frequency of 11.75kHz.

Figure 3. Photograph of NS-DBD *F*=1.712kHz, exposure time *t*=0.04s containing 68 pulses.

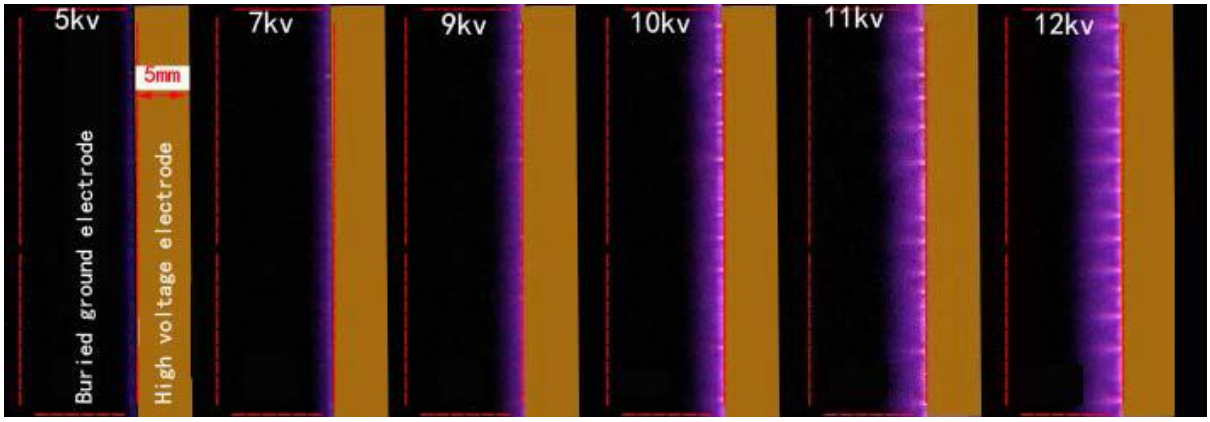

Figure 4. Photograph of AC-DBD *F*=11.75kHz, exposure time *t*=0.04s

C. Pressure Measurement System

The total 98 time-averaged pressure tappings are arranged in 3mm even increments, 7 row×14 columns. These pressure taps are arranged in a plexiglass board which is set vertical to the plasma actuator, as shown in Fig. 1. The model of pressure taps is 9816 by the PSI Company with a range -5000 to 5000 Pa and an accuracy of ±0.05% FS, which are read at frequency of 50 Hz and consecutive 10 seconds of sampling are performed for each case. As shown in Fig. 5.

The maximum of $|\Delta p|$ for all test cases is about equal to the maximum measurement error of 2.5 Pa. However, a study of the convergence of the time-averaged Δp validates the present measured results. In addition, total number of the pressure measurement channel is 96, which is not satisfied to all the orifices made in the static pressure board. So we just regard the Δp of the two most far-away orifices as zero.

In order to obtain more accurate data, another pressure measurement device called ND-8 micro-pressure transmitters is introduced to this experiment, whose range is -50 to 50Pa with an accuracy of 0.1%FS, better than that of PSI 9816. The experiment data acquisition frequency is 1000Hz and consecutive 10 seconds of sampling.

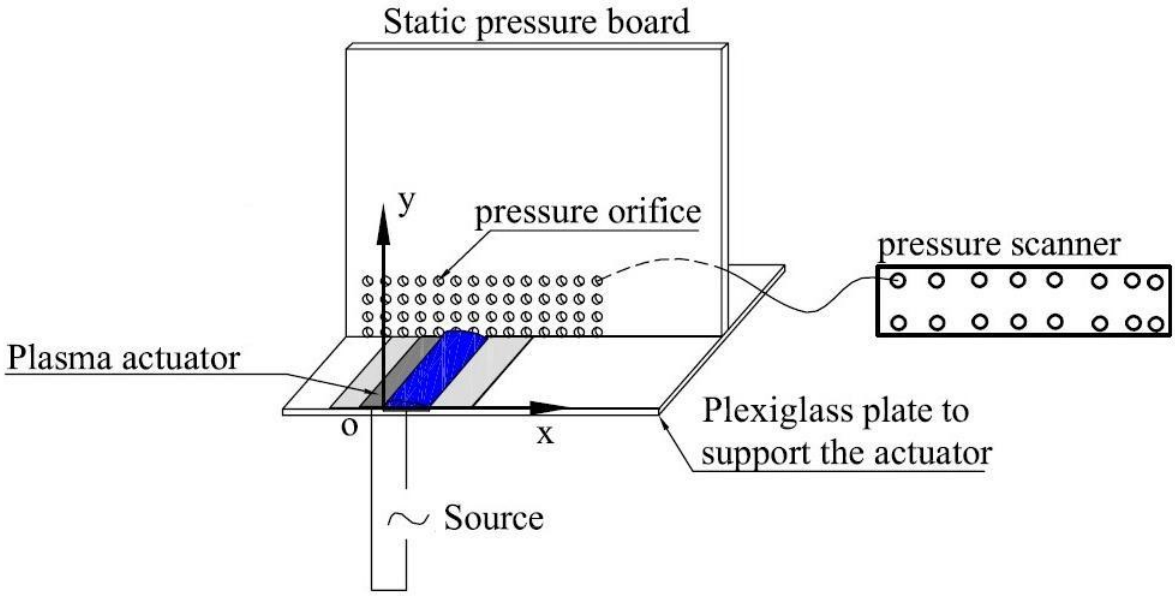

Figure 5. Sketch of the experimental pressure measurement setup for PSI 9816.

III. Experimental Results

In this part, the results of pressure increment, distributions of pressure increment along lines parallel to coordinate axes, and convergence of time-averaged pressure increment for the different control voltages will be plotted respectively.

A. Results for NS-DBD forcing at voltage V_{max}=6.88kV and frequency F=1.712kHz

1. Pressure Increment Contours

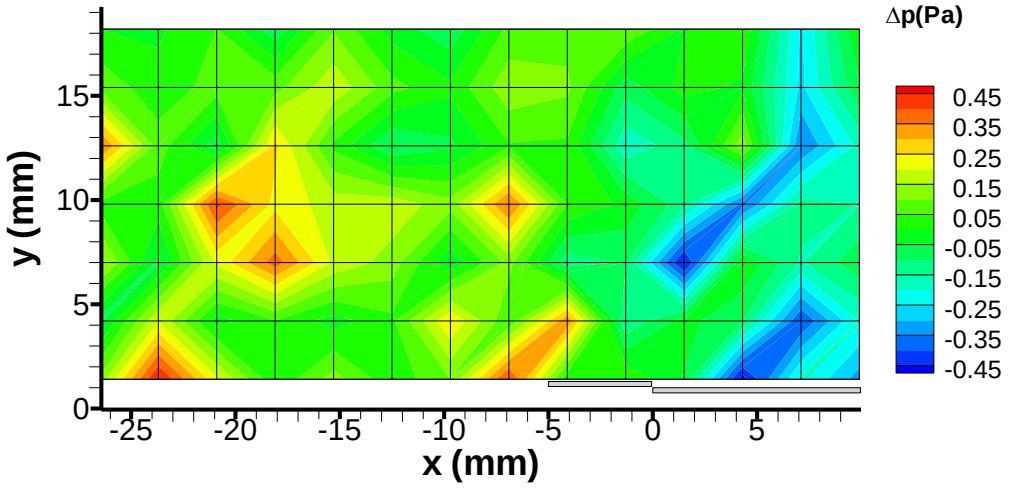

a) V_{max}=6.88kV

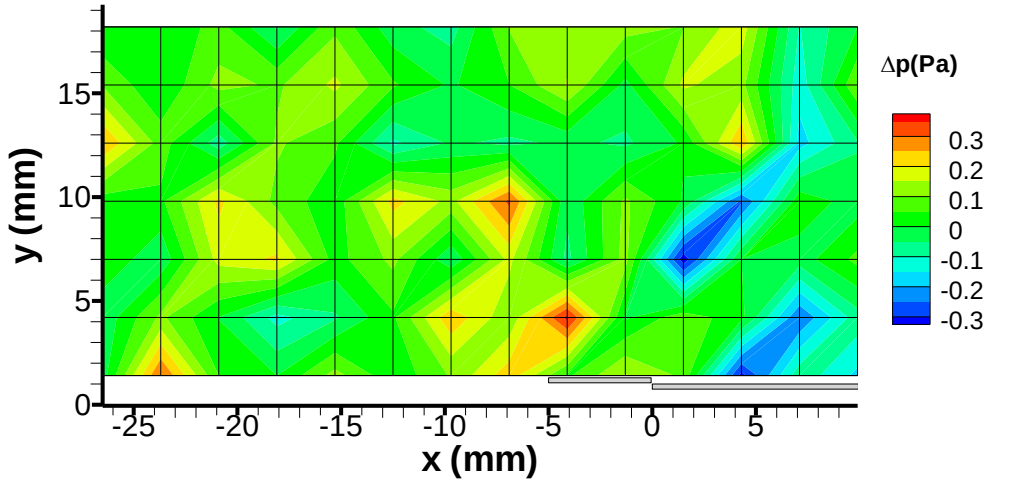

b) plasma-off

Figure 6. Pressure increment contour for NS-DBD forcing at V_{max}=6.88kV a) and plasma-off state b).

2. Distributions of Pressure Increment along Lines Parallel to Coordinate Axes

In this section, we select the max and min value from the contour above, to plot the distribution along lines parallel to coordinate axes through the points we selected. The positions of each points are shown in the Table 2 as follows.

Table 2. the position of the selected points for NS-DBD forcing at voltage V_{max}=6.88kV and frequency F=1.712kHz.

States	The position of max value		The position of min value	
	x (mm)	y(mm)	x(mm)	y(mm)
V_{max}=6.88kV	-23.7	1.4	4.3	1.4
Plasma-off state	-4.1	4.2	1.5	7.0

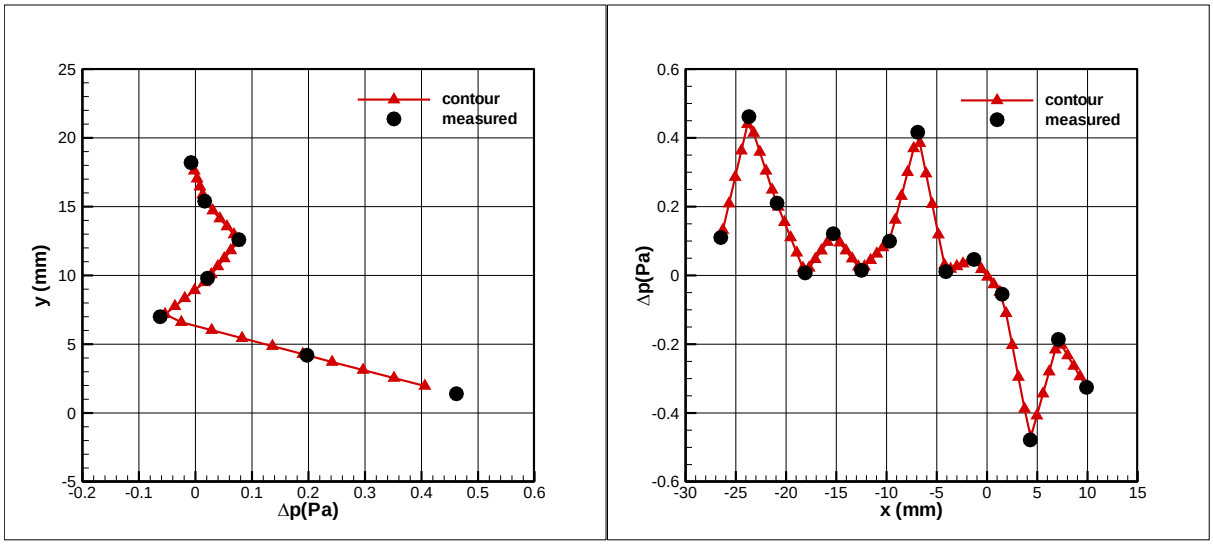

a) V_{max}=6.88kV

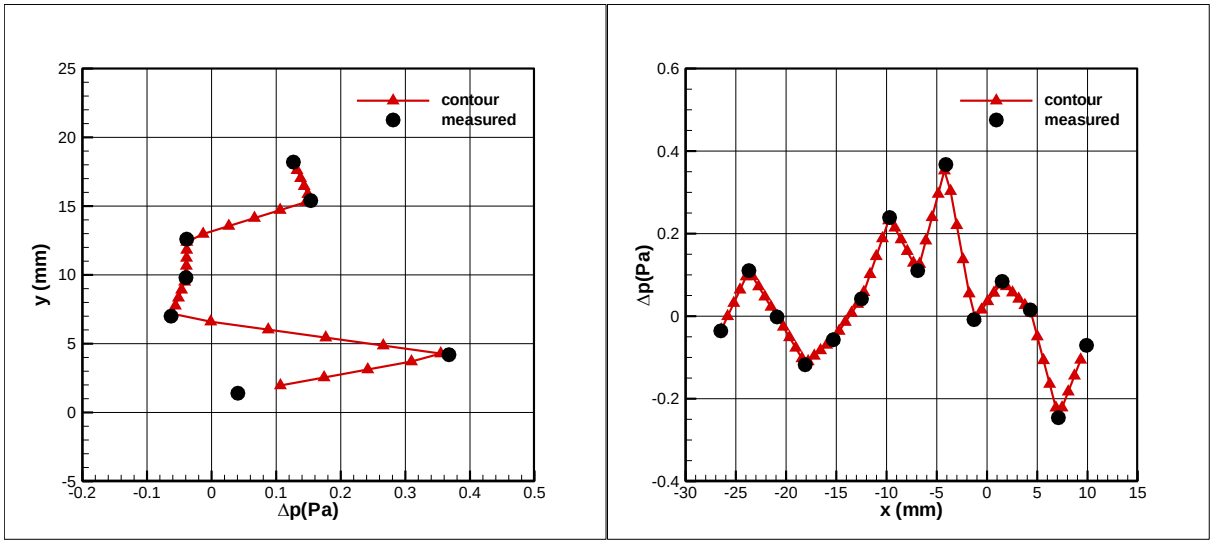

b) plasma-off

Figure 7. Distributions of pressure increment along lines parallel to coordinate axes for NS-DBD forcing at V_{max}=6.88kV a) and the plasma-off state b) through the max value point.

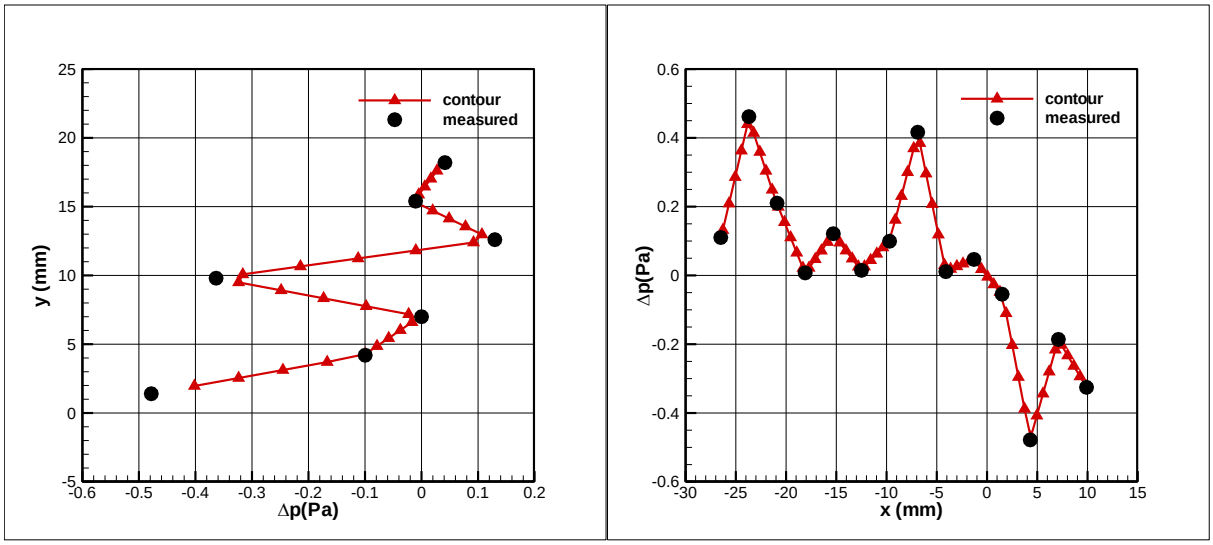

a) V_{max}=6.88kV

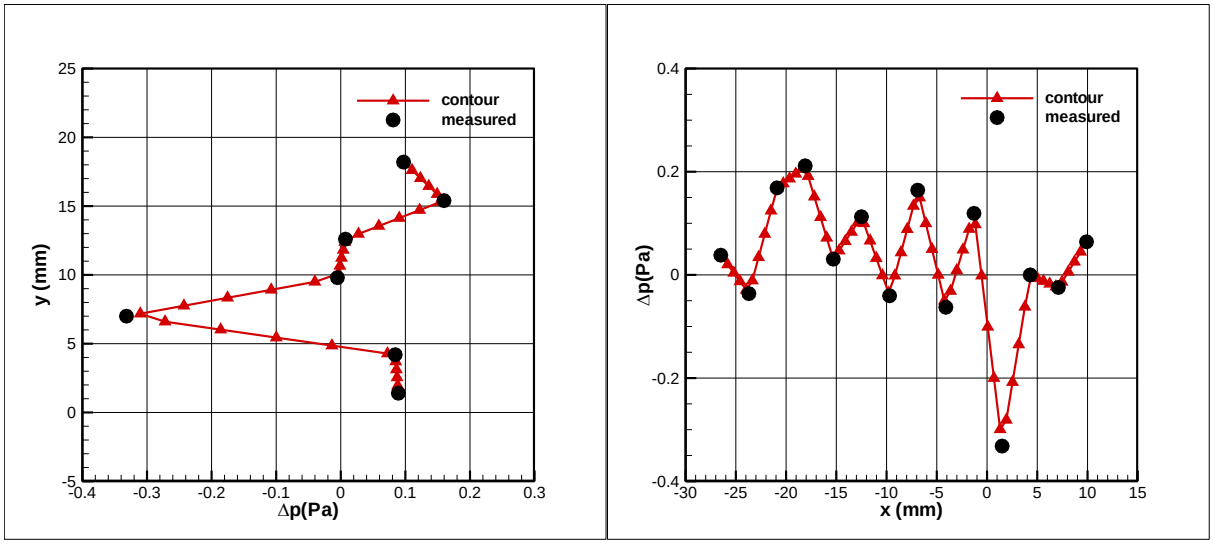

b) plasma-off

Figure 8. Distributions of pressure increment along lines parallel to coordinate axes for NS-DBD forcing at V_{max}=6.88kV a) and the plasma-off state b) through the min value point.

3. *Convergence of Time-Averaged Pressure Increment*

In this part, the convergence of the pressure increment through the max and min value will be plotted.

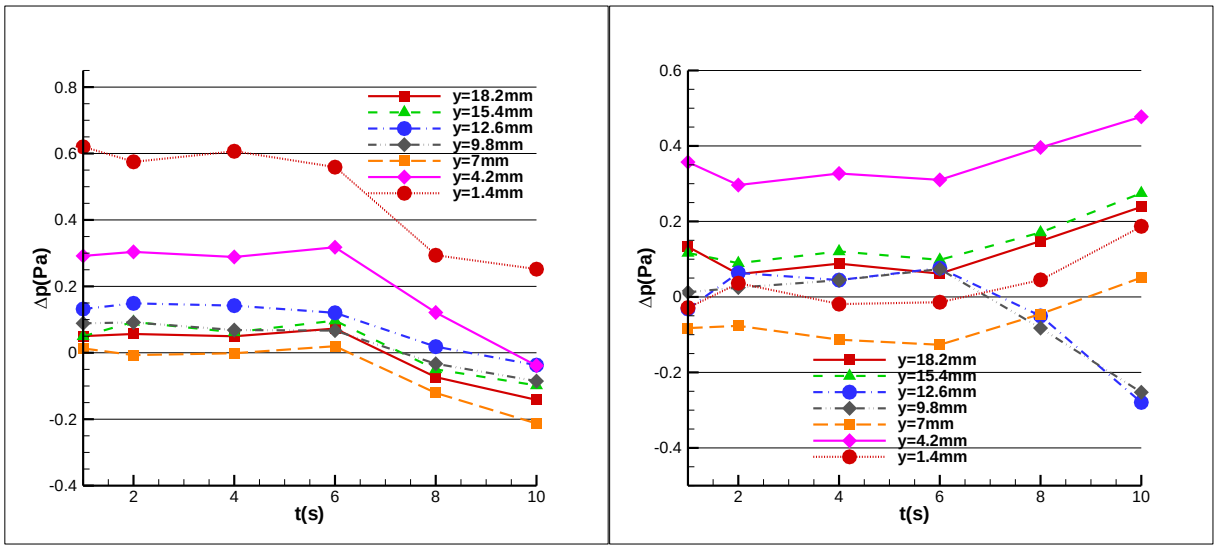

a) V_{max}=6.88kV b) plasma-off

Figure 9. The convergence of time-averaged pressure increment for NS-DBD forcing at V_{max}=6.88kV a) and the plasma-off state b) located at the max value.

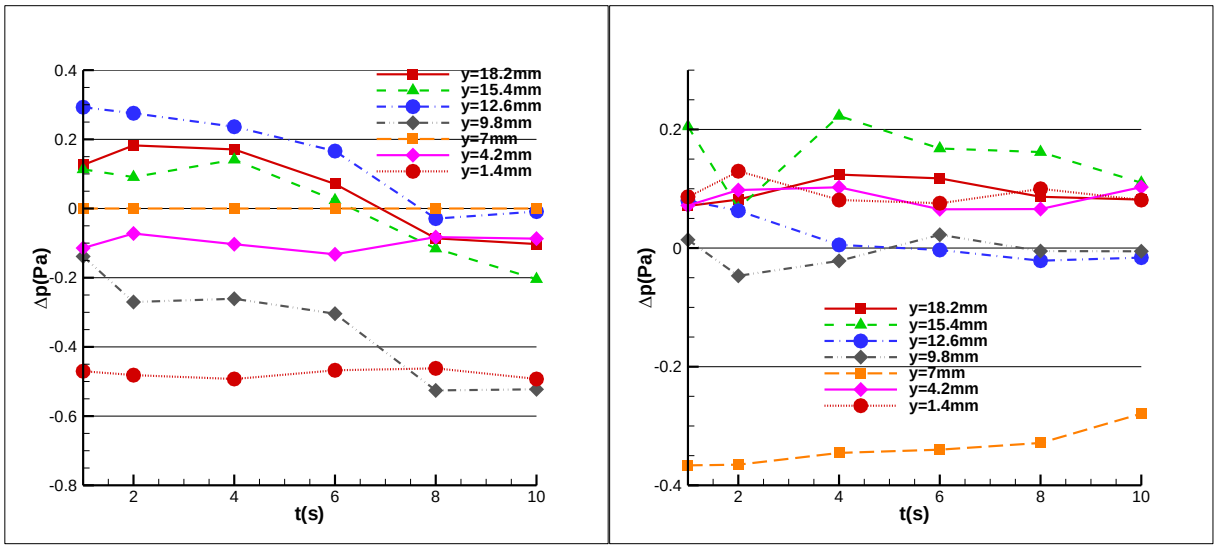

a) V_{max}=6.88kV b) plasma-off

Figure 10. The convergence of time-averaged pressure increment for NS-DBD forcing at V_{max}=6.88kV a) and the plasma-off state b) located at the min value respectively.

B. Results for NS-DBD forcing at voltage V_{max}=9.2kV and frequency F=1.712kHz

1. Pressure Increment Contours

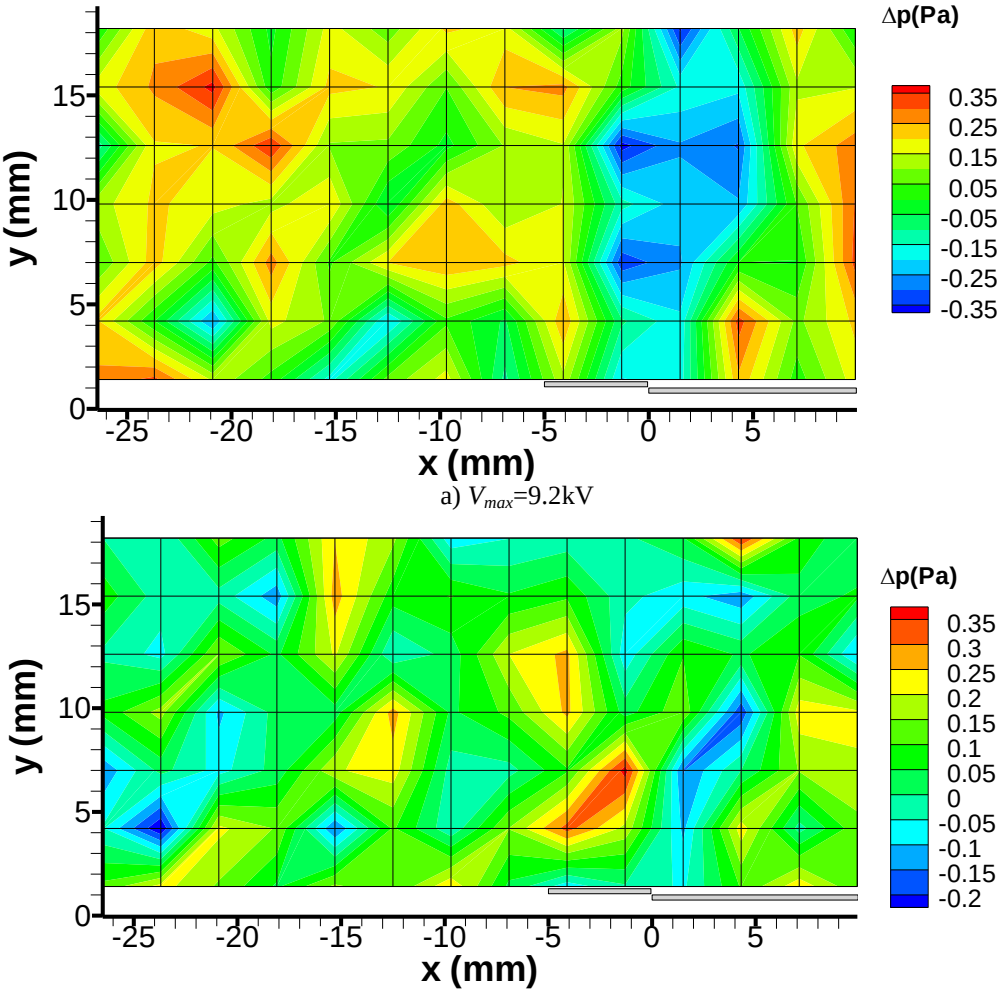

Figure 11. Pressure increment contour for NS-DBD forcing at V_{max}=9.2kV a) and plasma-off state b).

2. Distributions of Pressure Increment along Lines Parallel to Coordinate Axes

In this section, we select the max and min value from the contour above, to plot the distribution along lines parallel to coordinate axes through the points we selected. The positions of each points are shown in the Table 3 as follows.

Table 3. position of the selected points for NS-DBD forcing at voltage V_{max}=9.2kV and frequency F=1.712kHz.

States	The position of max value		The position of min value	
	x (mm)	y(mm)	x(mm)	y(mm)
V_{max}=9.2kV	-20.9	15.4	-1.3	12.6
Plasma-off state	9.9	7.0	-20.9	4.2

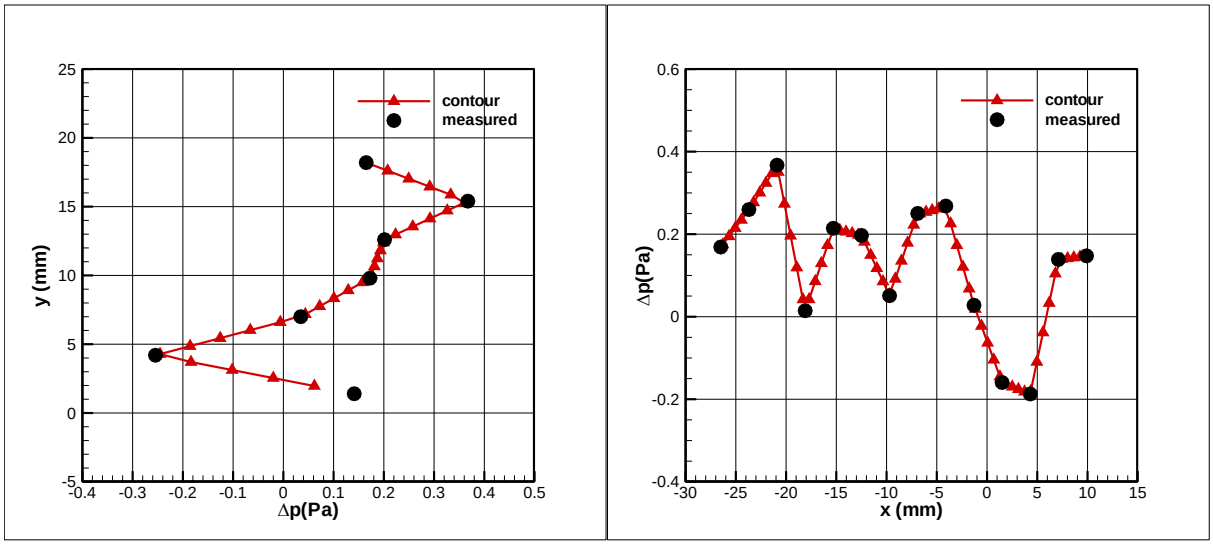

a) V_{max}=9.2kV

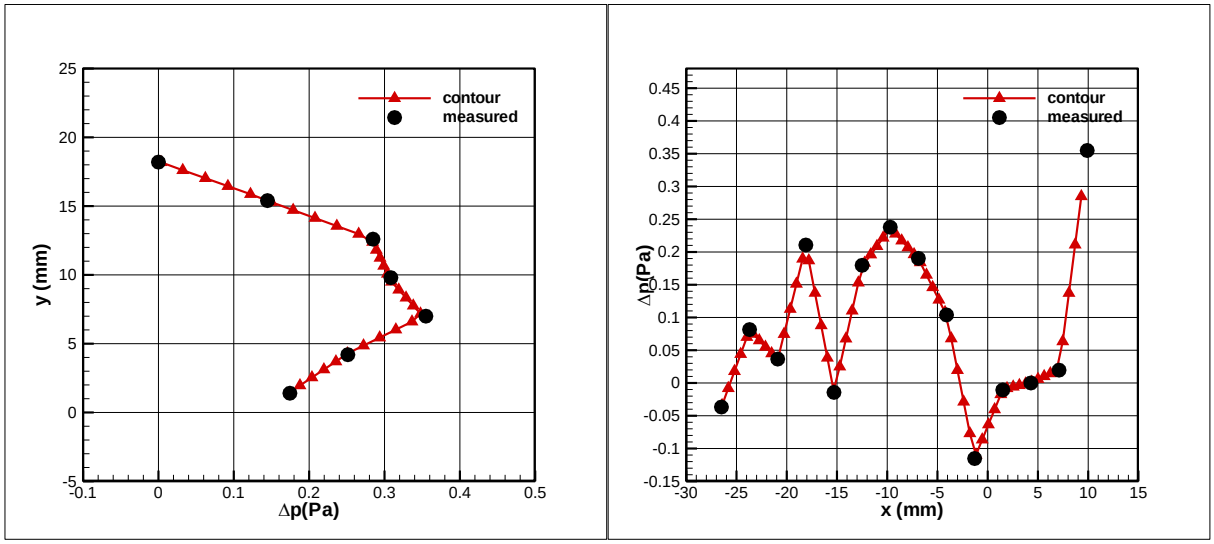

b) plasma-off

Figure 12. Distributions of pressure increment along lines parallel to coordinate axes for NS-DBD forcing at V_{max}=9.2kV a) and the plasma-off state b) through the max value point.

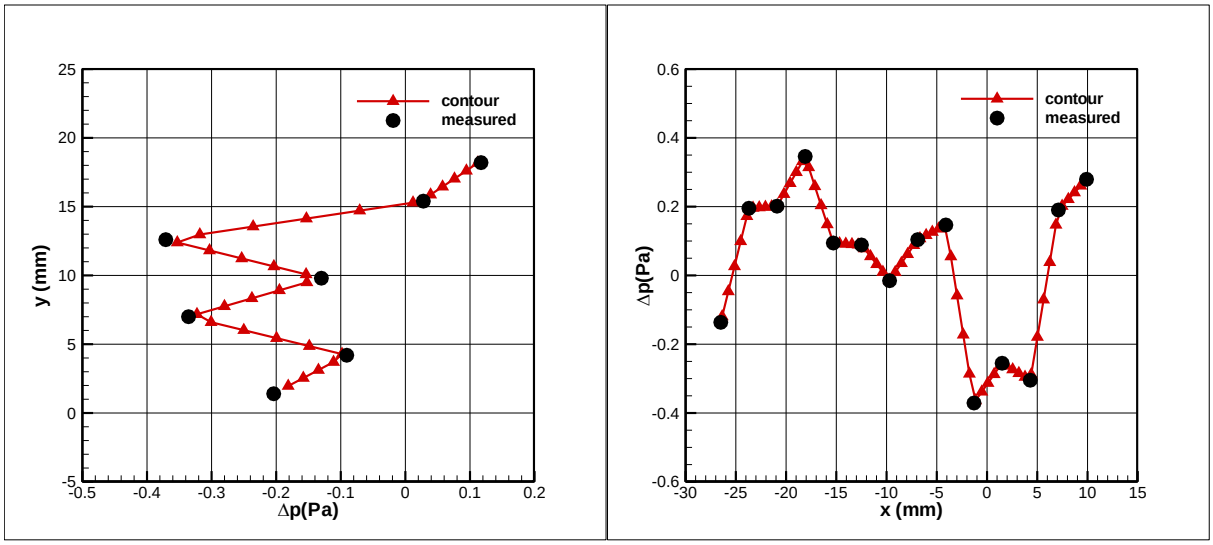

a) V_{max}=9.2kV

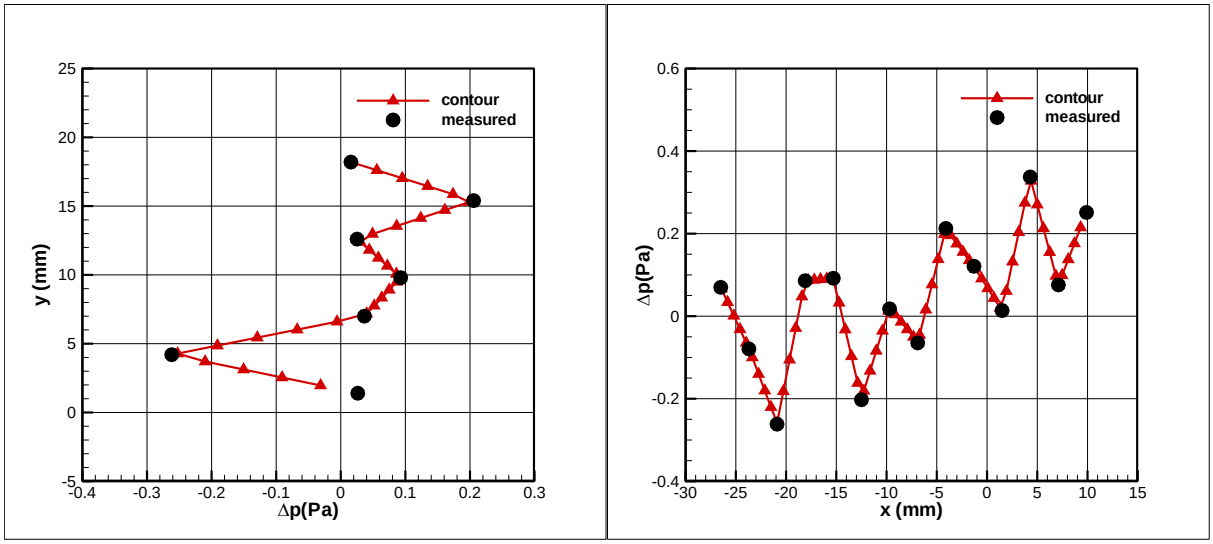

b) plasma-off

Figure 13. Distributions of pressure increment along lines parallel to coordinate axes for NS-DBD forcing at V_{max}=9.2kV a) and the plasma-off state b) through the min value point.

3. Convergence of Time-Averaged Pressure Increment

In this part, the convergence of the pressure increment through the max and min value will be plotted.

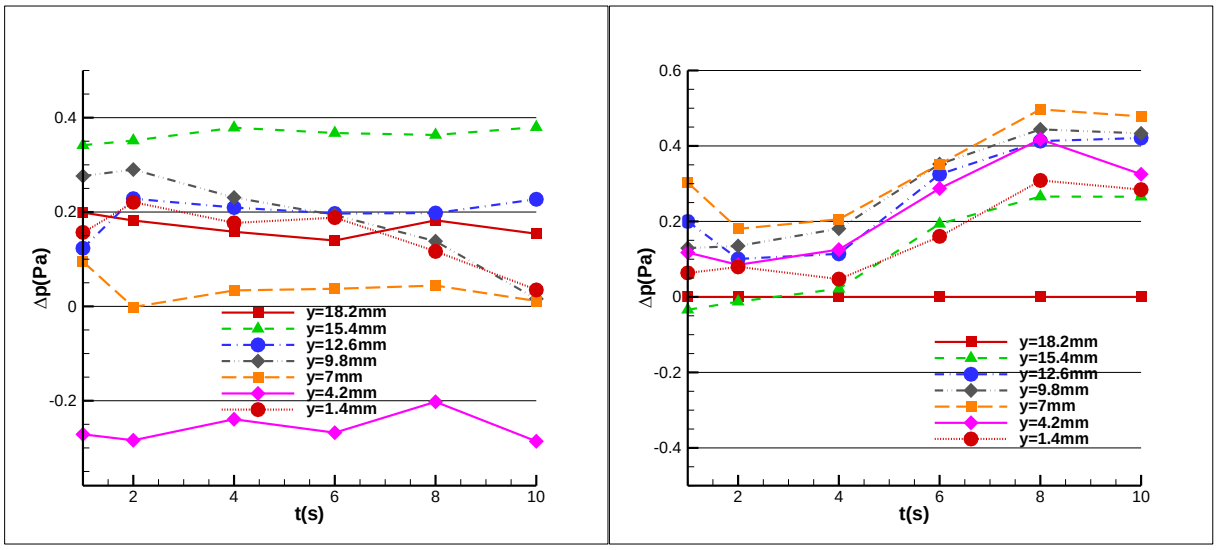

a) V_{max}=9.2kV b) plasma-off

Figure 14.The convergence of time-averaged pressure increment for NS-DBD forcing at V_{max}=9.2kV a) and the plasma-off state b) located at the max value.

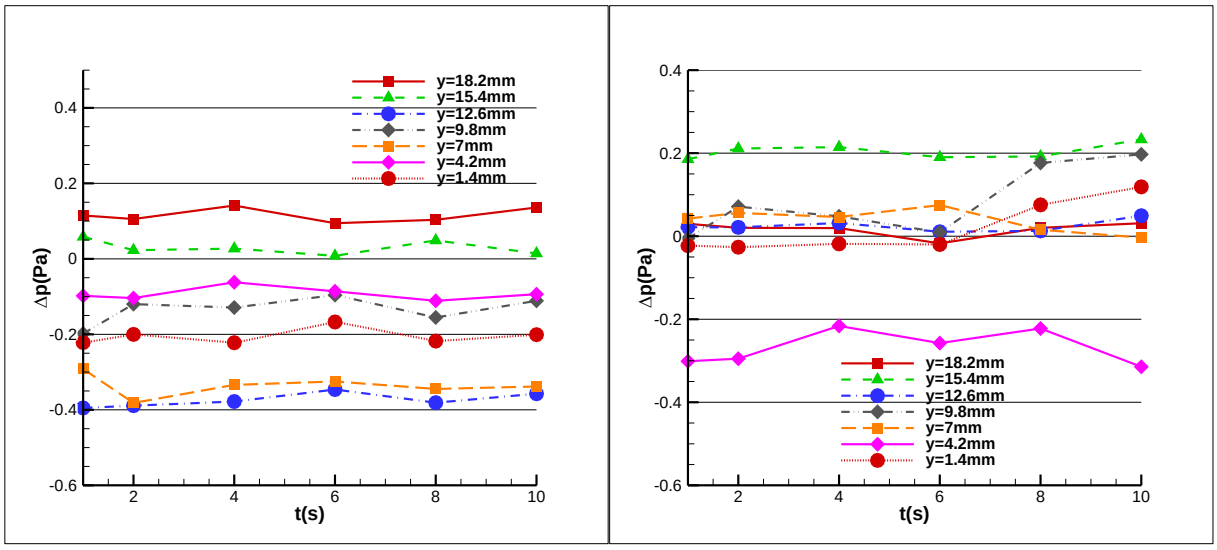

a) V_{max}=9.2kV b) plasma-off

Figure 15. The convergence of time-averaged pressure increment for NS-DBD forcing at V_{max}=9.2kV a) and the plasma-off state b) located at the min value respectively.

C. Results for NS-DBD forcing at voltage V_{max}=9.8kV and frequency F=1.712kHz

1. Pressure Increment Contours

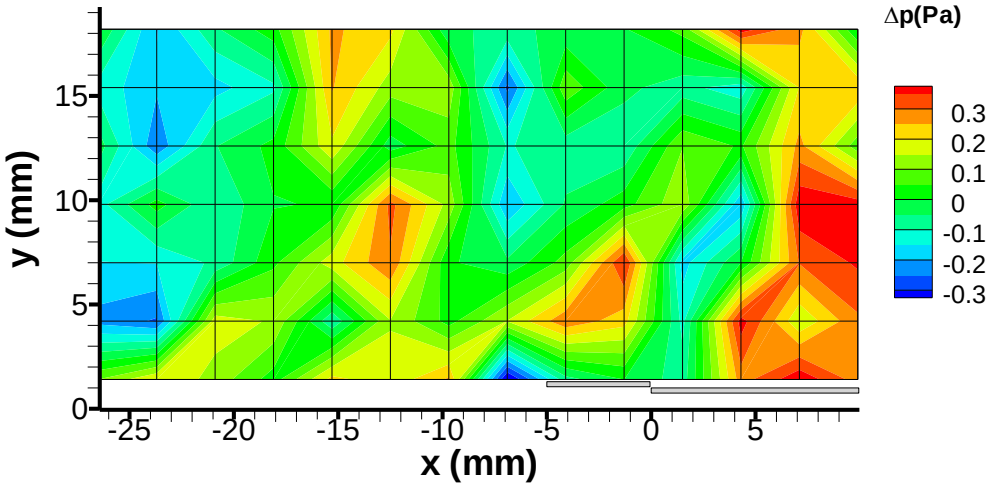

a) V_{max}=9.8kV

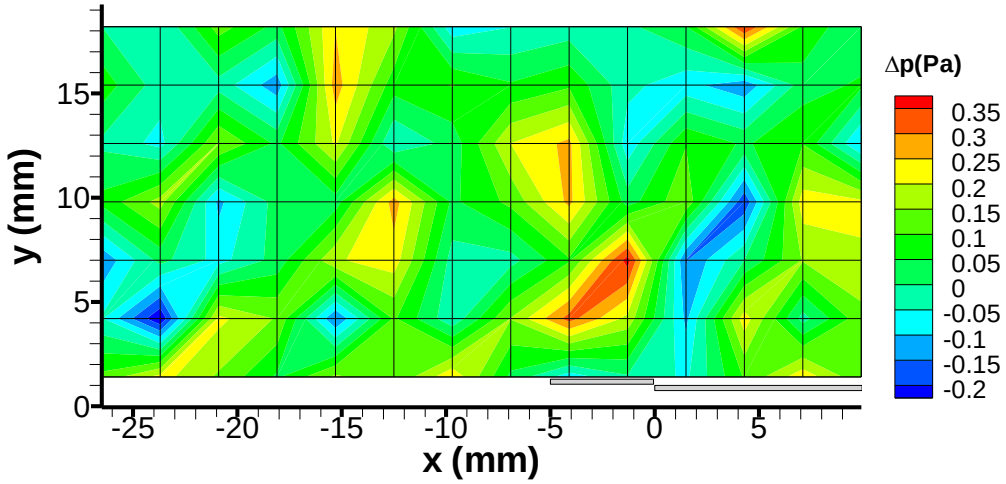

b) plasma-off

Figure 16. Pressure increment contour for NS-DBD forcing at V_{max}=9.8kV a) and plasma-off state b).

2. Distributions of Pressure Increment along Lines Parallel to Coordinate Axes

In this section, we select the max and min value from the contour above, to plot the distribution along lines parallel to coordinate axes through the points we selected. The positions of each points are shown in the Table 4 as follows.

Table 4. position of the selected points for NS-DBD forcing at voltage V_{max}=9.8kV and frequency F=1.712kHz.

States	The position of max value		The position of min value	
	x (mm)	y(mm)	x(mm)	y(mm)
V_{max}=9.8kV	7.1	9.8	-6.9	1.4
plasma-off state	-1.3	7.0	-23.7	4.2

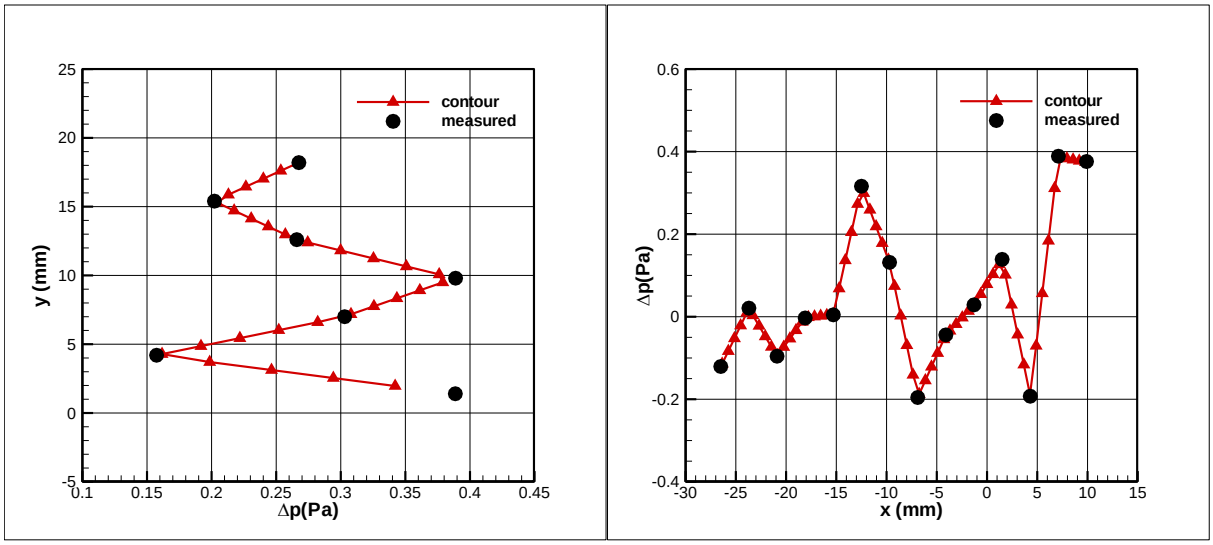

a) V_{max}=9.8kV

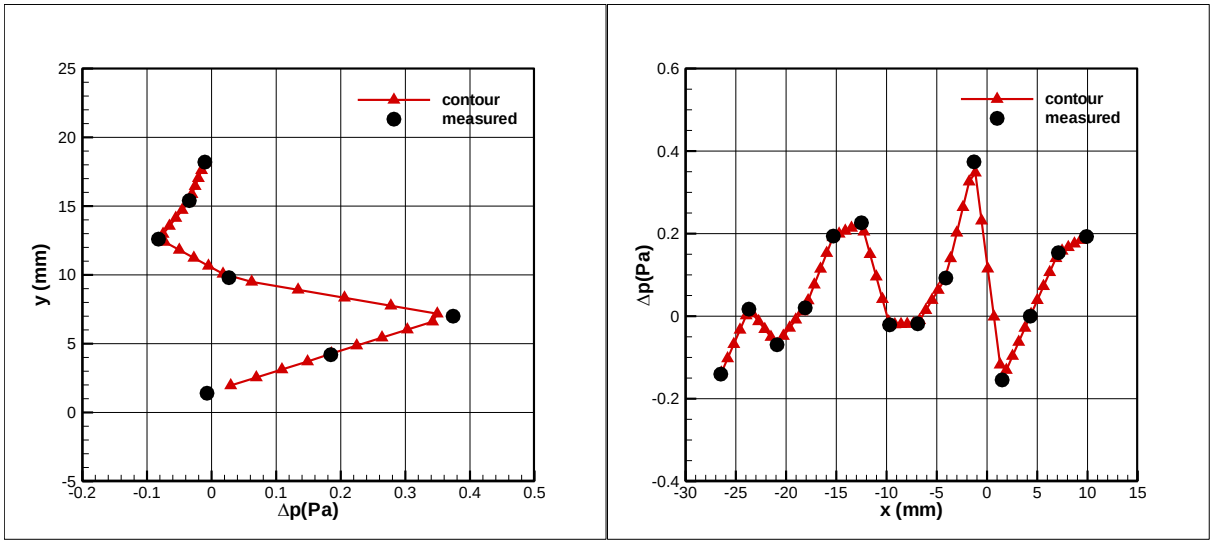

b) plasma-off

Figure 17. Distributions of pressure increment along lines parallel to coordinate axes for NS-DBD forcing at V_{max}=9.8kV a) and the plasma-off state b) through the max value point.

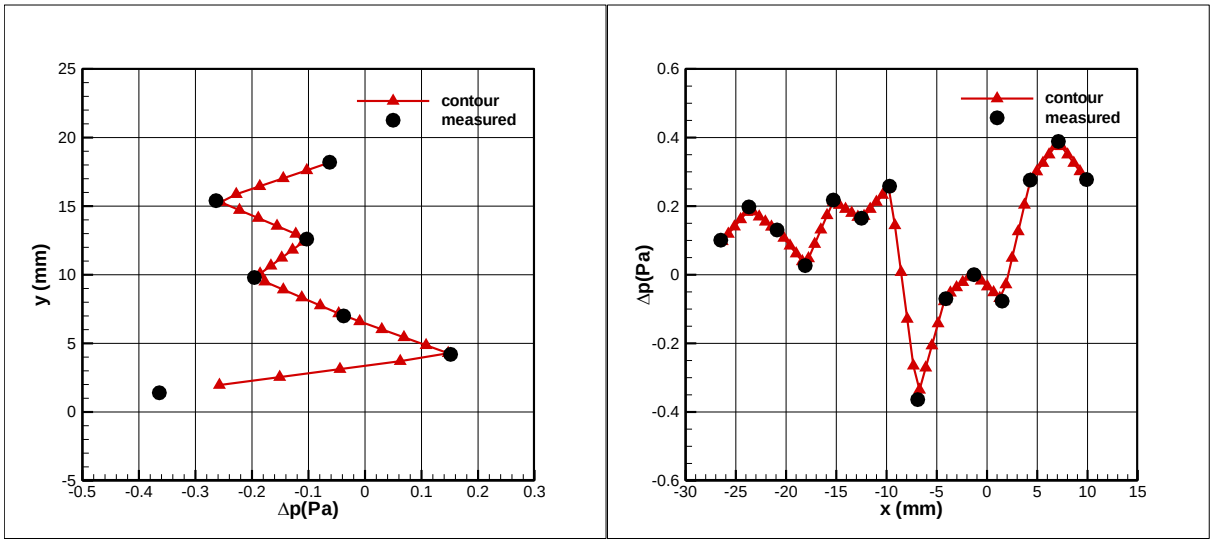

a) V_{max}=9.8kV

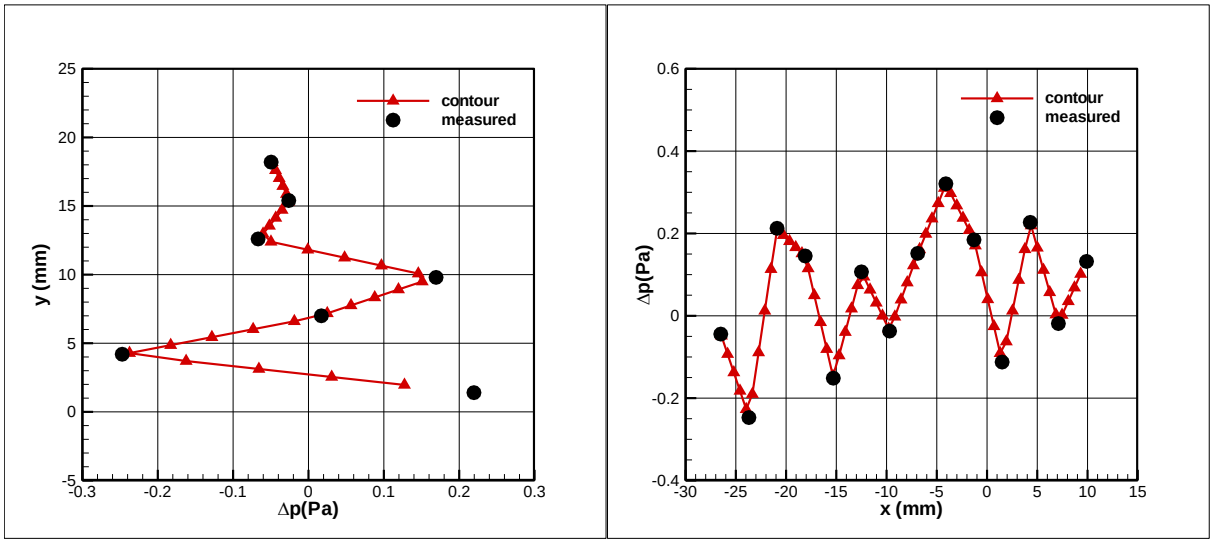

b) plasma-off

Figure 18. Distributions of pressure increment along lines parallel to coordinate axes for NS-DBD forcing at V_{max}=9.8kV a) and the plasma-off state b) through the min value point.

3. Convergence of Time-Averaged Pressure Increment

In this part, the convergence of the pressure increment through the max and min value will be plotted.

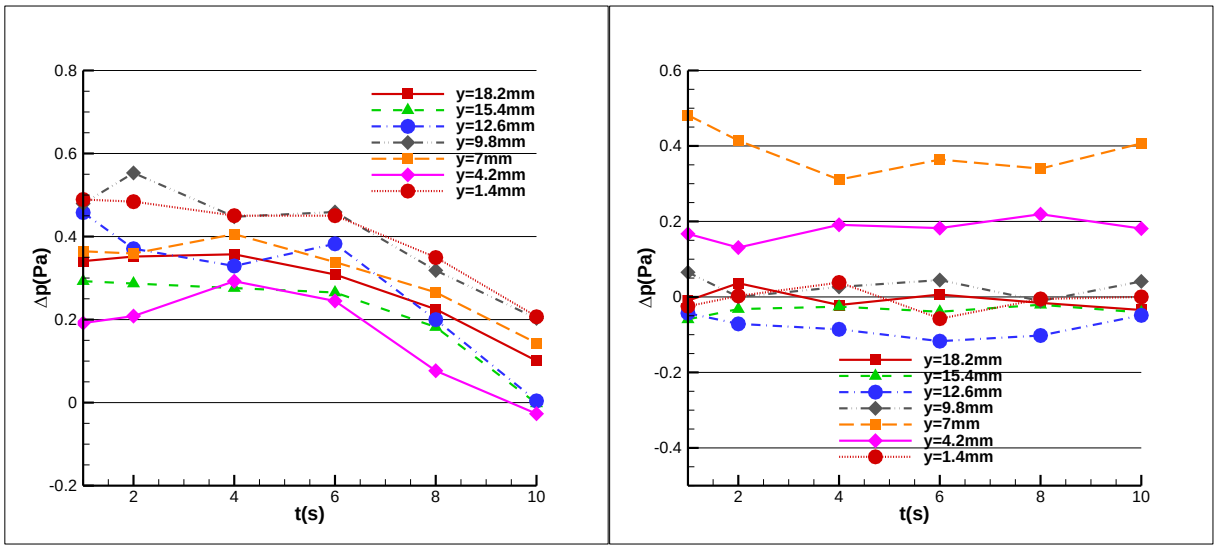

a) V_{max}=9.8kV b) plasma-off

Figure 19.The convergence of time-averaged pressure increment for NS-DBD forcing at V_{max}=9.8kV and the plasma-off state located at the max value.

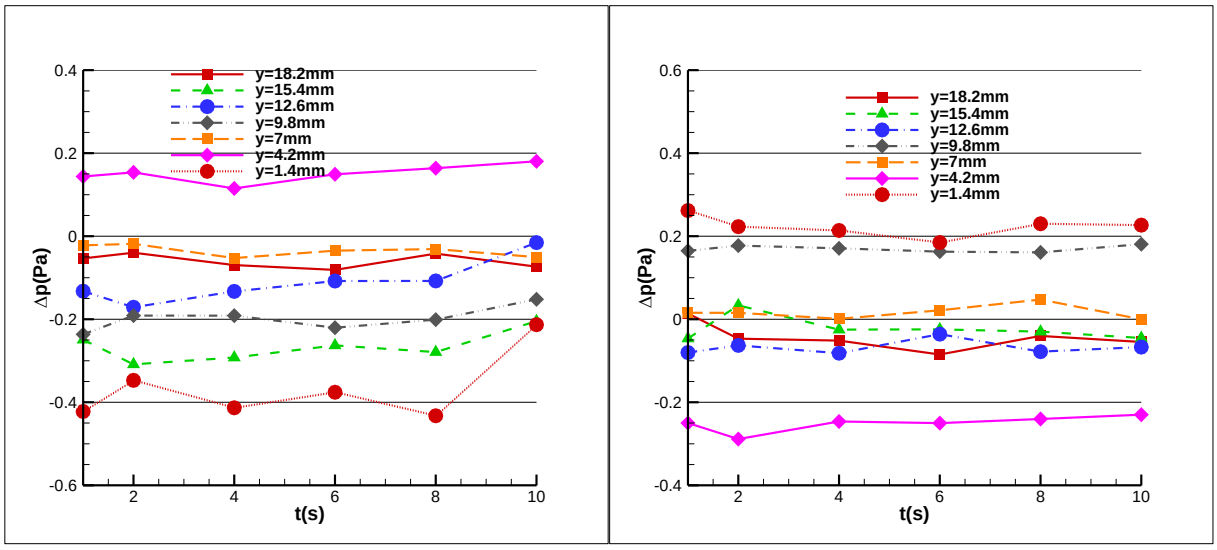

a) V_{max}=9.8kV b) plasma-off

Figure 20. The convergence of time-averaged pressure increment for NS-DBD forcing at V_{max}=9.8kV and the plasma-off state located at the min value respectively.

D. Comparison Part for AC-DBD

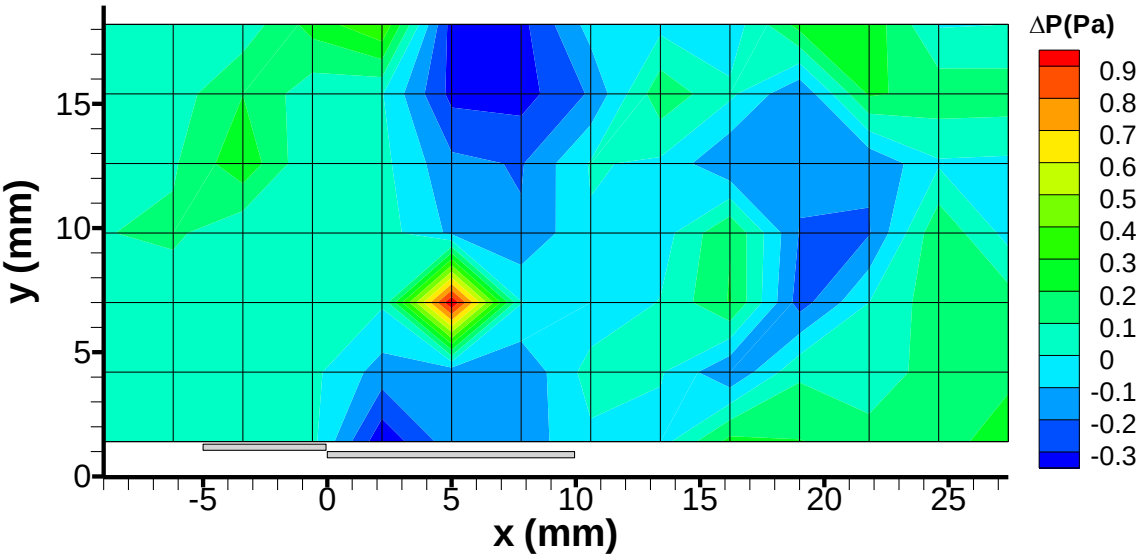

Figure 21. Pressure increment contour for AC-DBD forcing at $V_{P\text{-}P}$=12kV.

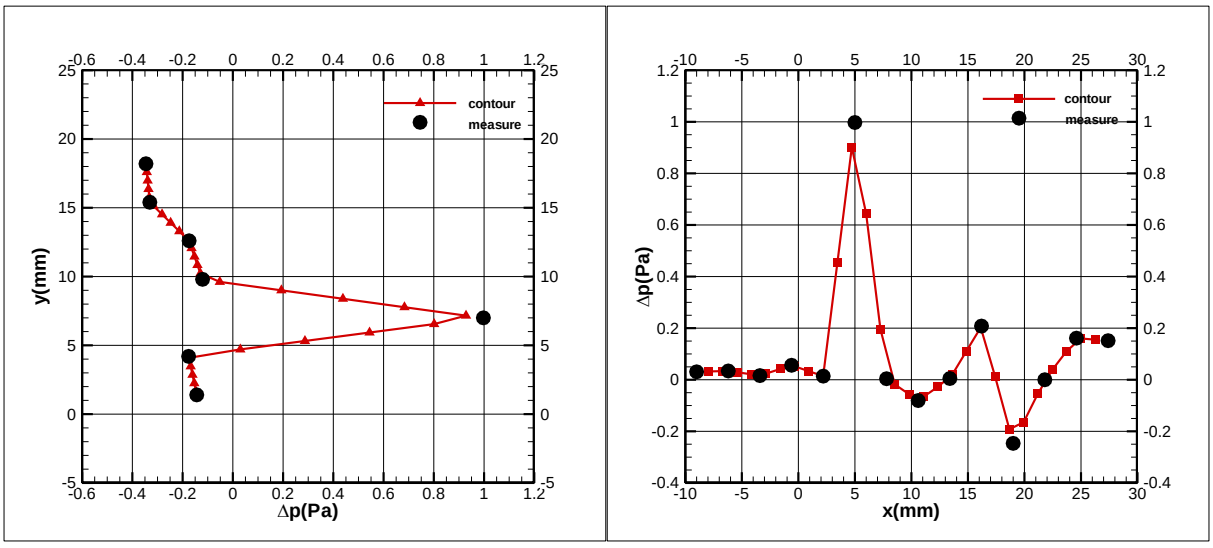

Figure 22. Distributions of pressure increment along lines parallel to coordinate axes for AC-DBD forcing at $V_{p\text{-}p}$=12kV through the max value point.

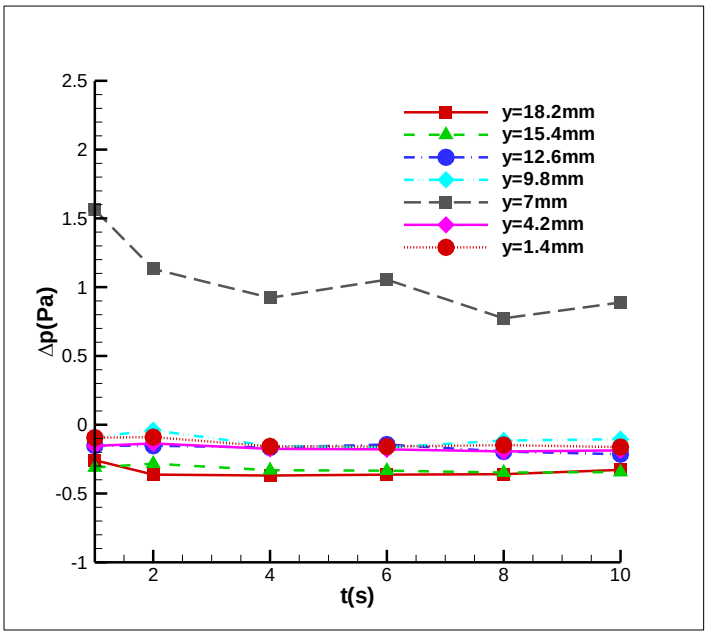

Figure 23.The convergence of time-averaged pressure increment for AC-DBD forcing at $V_{P\text{-}P}$=12kV located at the max value point.

E. Pressure distribution measured by ND-8 micro-pressure transmitters

In order to compare with the two different pressure sensor, we choose 2 same control voltages as before. For NS-DBD we select the control voltage V_{max}=9.8kV, for AC-DBD we select $V_{P\text{-}P}$=12kV. The final results are as follows.

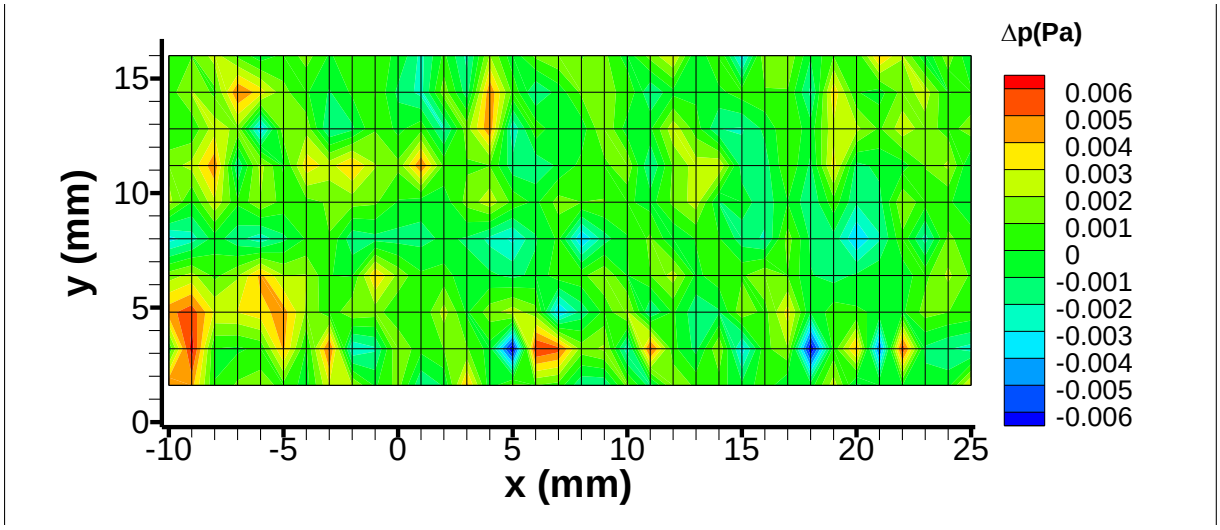

Figure 24.The pressure increment distribution measured by ND-8 micro-pressure transmitters at plasma off state.

Compare the range measured by ND-8 at the plasma off states (Figure 24) and that measured by PSI 9816, see figure 6.b), 11.b) , 16.b), we can conclude in according to the comparison results that the PSI 9816 is not accurate enough for this experiment. In general, the pressure increment is largely close to the value zero, which means the ND-8 is effective.

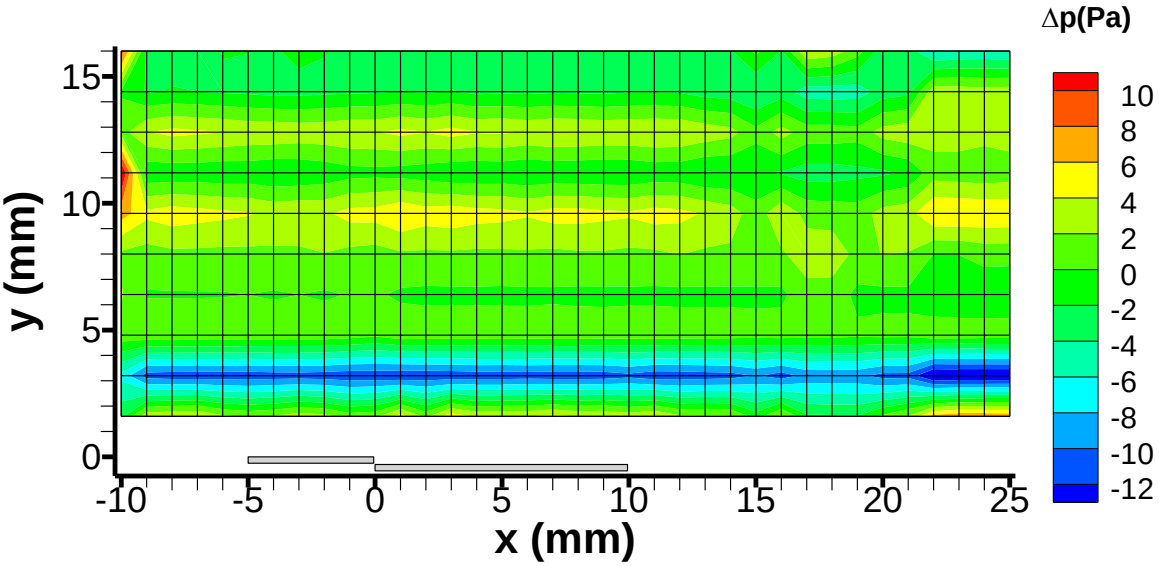

Figure 25. Pressure increment contour for AC-DBD forcing at $V_{P\text{-}P}$=12kV measured by ND-8 transient differential pressure sensors

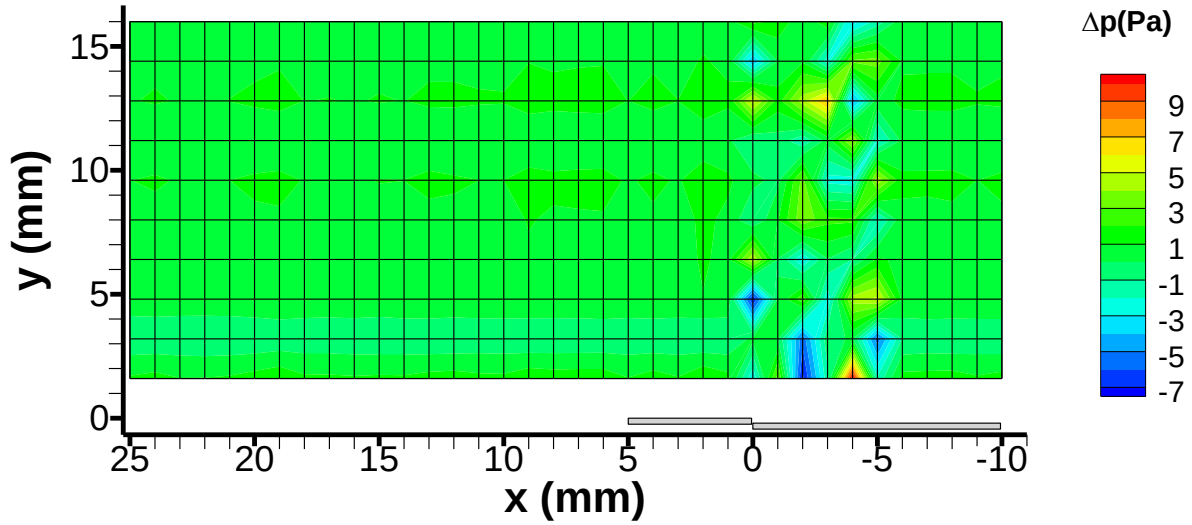

Figure 26.Pressure increment contour for NS-DBD forcing at V_{max}=9.8kV measured by ND-8 transient differential pressure sensors

As to the plasma on states, the results from PSI 9816 is nearly the same as that of plasma off states, however, the results from ND-8 shows significantly difference, which, may because of the effectiveness of the ND-8.

IV. Conclusions

The efficacy of dielectric barrier discharge (DBD) plasmas driven by repetitive nanosecond (NS) pulses for pressure distribution is investigated experimentally in quiescent air. Pressure increment distribution is measured by a PSI 9816 pressure scanner and the ND-8 micro-pressure transmitters. For the results measured by 9816, convergences of time-averaged pressure increment components are displayed to ensure the credibility of the data. A

parametric study on pressure distribution for NS-DBD is conducted for the max voltage value ranging from 6.88 kV to 9.8 kV at the carrier frequency of 1.712kHz in comparison with the results of AC-DBD conducted for the peak-peak 12.8kV at the carrier frequency of 11.75kHz. Results show that for the NS-DBD, the range of the pressure increment value of the plasma on and off state are almost the same. As to the data measured by PSI9816, it seems reliable with the convergence analysis; however, it's not correct in comparison with the data measured by ND-8. Due to time constraints, the experiments for ND-8 have not yet accomplished. Further work will mainly focus on pressure measurement with ND-8. And hope it will do some help to the bodyforce analysis.

The pressure increments induced by the plasma actuation measured by PSI 9816 transducer are not reliable, since the mearsured results, in general, have the same order of magnitude as the transducer accuracy and, moreover, the results for plasma-on and plasma-off are nearly of the same order of magnitude, although the convergences of the measurements are verified.

The innovative pressure measurement technique using micro-pressure transmitter ND-8 is shown for the first time to provide practically zero pressure increments for the plasma-off case and results greater than the transmitter accuracy for the plasma-on cases. This opens up exciting future research opportunities to inprove the computation of the body force field of dielectric barrier discharge actuators based on both PIV and pressure-field measurements . Future investigations should be pursued to refine the measurement technique of the ND-8 transmitters.

References

[1]Corke, T., Post, M. and Orlov, D., "Single Dielectric Barrier Discharge Plasma Enhanced Aerodynamics: Physics, Modeling and Applications," *Experiments in Fluids*, Vol. 46, 2009, pp.1-26.

[2]Moreau, E., "Airflow Control by Non-Thermal Plasma Actuators," Journal of Physics D: Applied Physics, Vol. 40, 2007, pp. 605-636.

[3]Forte, M., Jolibois, J., Moreau, E., Touchard, G. and Cazalens, M., "Optimization of a Dielectric Barrier Discharge Actuator by Stationary and Non-Stationary Measurements of the Induced Flow Velocity: Application to Airflow Control," *Experiments in Fluids*, Vol, 43, 2007, pp. 917-928.

[4]Corke, T., Enloe, C. and Wilkinson, S., "Dielectric Barrier Discharge Actuators for Flow Control,"*Annual Review of Fluid Mechanics*, Vol. 42,2010pp. 505-529.

[5]Roupassov, D., Likhanskii, A., Mudnova, M. and Starikovskii, A.," Flow Separation Control of High-Speed and High-Actuator in Air," *Journal of Fluid Mechanics*, Vol, 103, No. 053305, 2008, pp 1-13.

[6]Opaits, D., Likhanskii, A., Neretti, G., Zaidi, S., Shneider, M., Miles, R. and Macheret, S., "Experimental Investigation of Dielectric Barrier Discharge Plasma Actuators Driven by Repetitive High-Voltage Nanosecond Pulses with DC or Low Frequency Sinusoidal Bias," *Journal of Applied Physics*, Vol. 104, No. 043304, 2008, pp. 1-15.

[7]Likhanskii, A., Shneider, M., Macheret, S. and Miles, R., "Modeling of Dielectric Barrier Discharge Plasma Actuator in Air," *Journal of Applied Physics*, Vol. 103, No. 053305, 2008, pp. 1-13.

[8]Xuanshi Meng., Yushuai Wang., Jianlei Wang., Jinsheng Cai., et al.," Body Force Produced by Plasma Actuator Using PIV and Pressure Measurements" *AIAA 51st Aerospace Science Meeting*, AIAA Paper 2013-0396, 2013.